ACES Asian Chemical Editorial Society

doi.org/10.1002/asia.202100419

CHEMISTRY AN ASIAN JOURNAL Full Paper

Symmetry Breaking and Autocatalytic Amplification in Soai Reaction Confined within UiO-MOFs under Heterogenous Conditions.

Giuseppe Rotunno,[a, b] Gurpreet Kaur,[a, b] Andrea Lazzarini,[a, b] Carlo Buono,[a, b] and Mohamed Amedjkouh*[a, b]

Abstract: Symmetry breaking is observed in the Soai reaction in a confinement environment provided by zirconium-based UiO-MOFs used as crystalline sponges. Subsequent reaction of encapsulated Soai aldehyde with $Zn(i\text{-}Pr)_2$ vapour promoted absolute asymmetric synthesis of the corresponding alkanol. ATR-IR and NMR confirm integration of aldehyde into the porous material, and a similar localization of newly formed chiral alkanol after reaction. Despite the confinement, the Soai reaction exhibits significant activity and autocatalytic amplification. Comparative catalytic studies with various UiO-MOFs indicate different outcomes in terms of enantiomeric excess, handedness distribution of the product and reaction rate, when compared to pristine solid Soai aldehyde, while the crystalline MOF remains highly stable to action of $Zn(iPr)_2$ vapour. This is an unprecedented example of absolute asymmetric synthesis using MOFs.

1. Introduction

Chirality remains an intriguing scientific topic. Biomolecules in nature exhibit overwhelming one-handedness, often called homochirality, such as L-amino acids and D-sugars. Asymmetric catalysis can lead to the synthesis of enantiomerically pure chiral products in areas such as fine-chemicals and pharmaceuticals with growing need in the last decades. The asymmetry can be introduced through a chiral auxiliary or a chiral catalyst.[1] In contrast with asymmetric catalysis, in which the structures of catalyst and product are different, in asymmetric autocatalysis a chiral product acts as chiral catalyst for its own production.[2] The Soai reaction remains a remarkable example of amplifying asymmetric autocatalysis.[3,4] The addition of $Zn(i\text{-}Pr)_2$ to a rigid pyrimidine-5-carbaldehydes such as **1** in toluene provides alkanols **2** with increasing ee.[5] Furthermore, it showed to be prone to amplification of ee despite the absence of the corresponding alcohol **2**, but in presence of various chiral factors[6] and, even more strikingly, in absence of any chiral substance.[7] Recently, asymmetric amplification of such autocatalysts was realized under heterogenous phase, *via* a heterogeneous vapour-solid interaction, by reaction of *iPr_2Zn vapor on achiral solid aldehyde*.[8] The synthesis of optically active compounds from achiral precursors has been defined as absolute asymmetric synthesis.[9]

In search for a validate mechanism of the remarkable asymmetric amplification efforts have been made using advanced techniques such as microcalorimetry,[10] NMR analysis[11] and DFT calculations.[12] These analyses revealed the presence of dimers, tetramers and even higher-level aggregates in the reaction cycle. Combinatory studies of NMR and DFT techniques[13,14] and XRD analysis of crystals[15] added support for these findings (Figure 1). Gridnev *et al.* have computationally quantified the abundance of the species in the reaction pool.[13] Dimers were proposed as the resting state of the catalyst, while tetramers were found as the active catalytic species. An alternative mechanism involves hemiacetal complexes, first observed as transient intermediates,[16] then by formation of subsequent derivatives under heterogenous conditions[8b] and further by *in situ* mass spectroscopic investigations.[17] Nevertheless, as proposed by Brown et al.,[11c] once the reaction provides a tiny enantiomeric imbalance in the products, the *ee* can easily be propagated and amplified by the oligomerization of the reaction species.[18] Under homogeneous conditions, the dimers and tetramers involved in the reaction mechanism can diffuse in solution, propagate and even associate into indefinite polymers. In more recent investigations, Denmark *et al.* report on the function of the pyridyl- and pyrimidyl-moiety in the NMR studies revealing a tetrameric structure, also described as a cube escape model.[19]

Furthermore, the process is amenable to spontaneous molecular symmetry breaking under heterogeneous conditions by reaction of iPr_2Zn vapor-phase on solid aldehyde **1**.[20] Thus, in absence of solvent and with limited dynamic freedom the assembly and propagation of the reaction intermediates remains possible and allows for amplification in a constrained solid state. Therefore, it is relevant to probe confinement effects

[a] G. Rotunno, G. Kaur, Dr. A. Lazzarini, Dr. C. Buono, Prof. Dr. M. Amedjkouh
Department of Chemistry
University of Oslo
P.O. Box 1033, Blindern, 0315 Oslo (Norway)

[b] G. Rotunno, G. Kaur, Dr. A. Lazzarini, Dr. C. Buono, Prof. Dr. M. Amedjkouh
Center for Materials Science and Nanotechnology (SMN)
Faculty of Mathematics and Natural Sciences
University of Oslo
P.O. Box 1126, Blindern, 0318 Oslo (Norway)
E-mail: mamou@kjemi.uio.no

Supporting information for this article is available on the WWW under https://doi.org/10.1002/asia.202100419

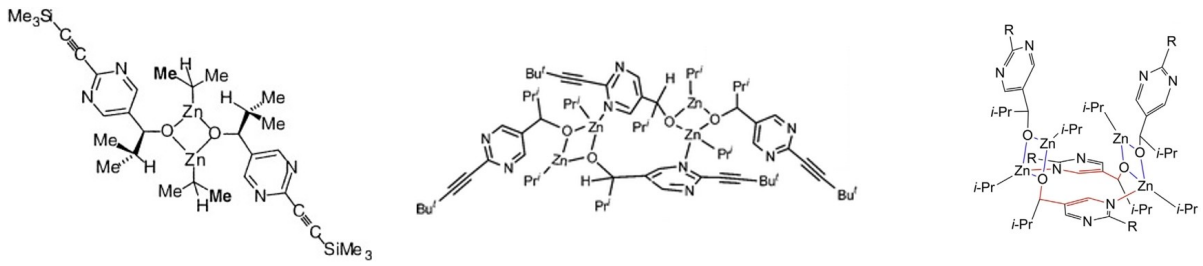

Figure 1. Selection of proposed or isolated reaction intermediates.

on the formation of the autocatalytic species and the extent of amplification if possible. Metal-Organic Frameworks (MOFs) provide an adequate environment as crystalline sponge for guest inclusion for such heterogenous asymmetric catalysis and perform asymmetric reactions in a pocket-like confined space. MOFs are porous crystalline materials, consisting of a 2D or 3D network, with metal containing nodes known as secondary building units (SBUs) linked by multidentate organic ligands (linkers) by strong chemical bonds.[21] They emerged as promising materials for various application such as catalysis, sensing, adsorption and separation due to their high porosity and large surface area and can be considered as nanoreactors. In the last decade, researchers have applied a variety of synthetic strategies to build chiral MOFs for asymmetric catalysis and a large number of MOF-catalysed organic reactions have been reported.[22] Herein, we present our study of the confinement of aldehyde **1** within the framework of MOFs functioning as nanocontainers/reactors. Consequently, the oligomerization is subject to mesoporosity of the framework, which enforces limited propagation of the reaction intermediates through channel openings. To this end, it is imperative to probe MOFs with various open channels and linker functionalities because of the need to transport typically very large organic substrates and products. This effect could significantly influence the final conversion and enantiopurity of Soai alcohol **2** in the reaction.

Because of the spontaneous symmetry breaking in the Soai reaction, there was no need of a chiral MOF as asymmetric inductor/catalyst for our studies. The materials of our choice were UiO-type MOFs, namely UiO-66 and UiO-67, consisting of a metal cluster of 6 Zr(IV) ions arranged in an octahedron and, respectively, the organic linkers terephtalic acid (H_2bdc) and biphenyl-4,4′-dicarboxilic acid (H_2bpdc) (Figure 2). To the best of our knowledge, this is the first example of absolute asymmetric autocatalysis performed within *"achiral"* MOF.

2. Inclusion

2.1. Preliminary DFT calculations

Periodic DFT calculations have been performed in order to predict the position in which Soai aldehyde **1** would preferentially be allocated inside UiO-67 and UiO-66 (Figure 3). Firstly,

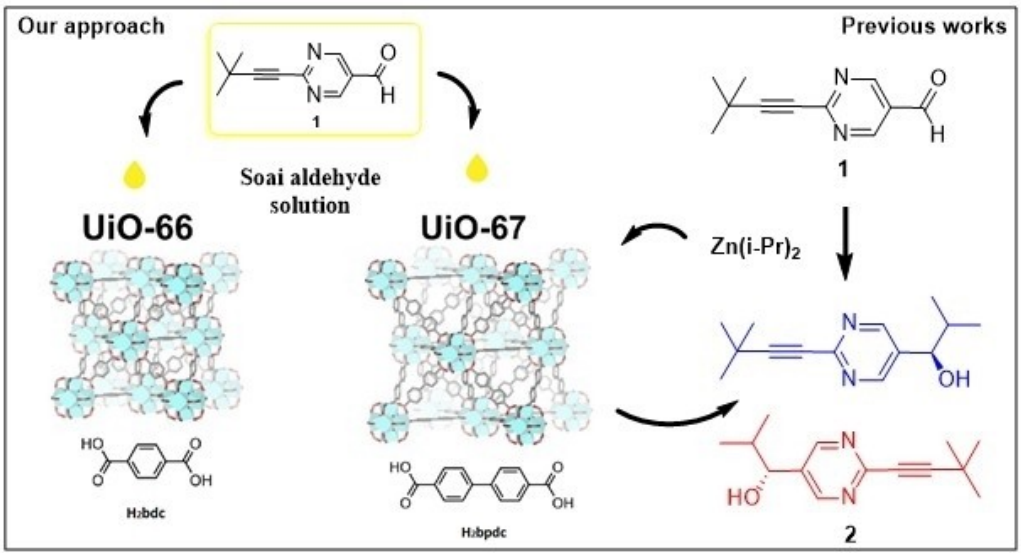

Figure 2. Schematic outline of guest inclusion in UiO-MOFs.

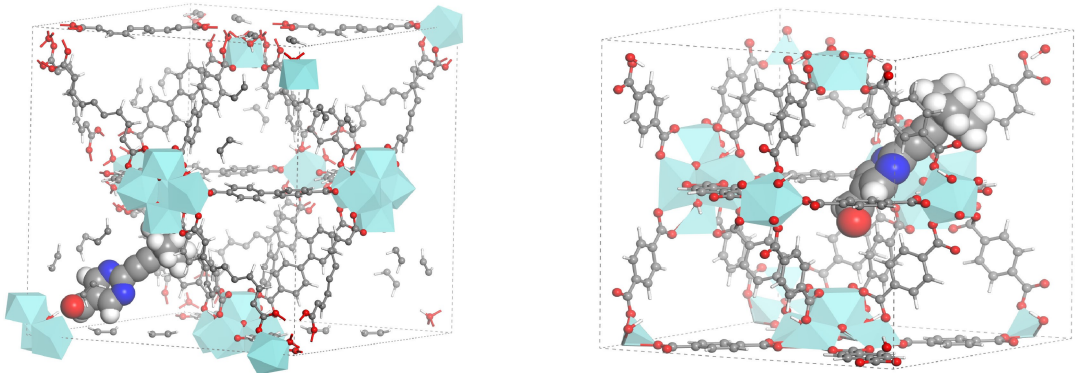

Figure 3. Periodic DFT calculations of **1** in cavities of UiO-67 (left) and UiO-66 (right).

comparing the structures of **1** and the linkers of the two MOFs, the size of the aldehyde (10.5 Å) was found slightly smaller than the size of the biphenyl dicarboxylate linker of UiO-67, while terephtalic acid linkers of UiO-66 were almost half the size of the aldehyde. (See SI). The octahedral cages of the MOFs have been calculated being 16 Å for UiO-67 and 11 Å for UiO-66.[23]

In UiO-67, the optimized structure shows **1** physiosorbed in the octahedral cage of the framework, with the formation of an H-bond between the hydrogen of the hydrated cornerstone of the MOF cluster and the oxygen of the carbonyl group of the aldehyde. In the UiO-66 the cavity of the MOF is too small for the allocation of aldehyde **1** in the same position as in UiO-67. The most stable structure predicts the aldehyde inside the cavity establishing only weak van der Walls interactions with the organic linkers.

2.2. The inclusion process

The inclusion of Soai aldehyde **1** has been performed by soaking sample of MOF powder in a toluene solution of **1** (Figure 2). We carried out tests with varying the ratio between aldehyde and MOF (0.5:1, 1:1, 2:1), which led to the optimized ratio in weight between MOF and aldehyde **1** being 1:2 to provide better HPLC analysis. The solution evaporated at r.t.: the slow evaporation of the solvent gradually concentrates the guest, which diffuses by capillary absorption and crystallizes inside the pores of the host.[24] After complete evaporation, the MOF powder was washed and filtered under vacuum with acetone and oven-dried at 140 °C. The washing process is a key step that removes the excess of **1** present on the surface of the MOF, unbound to the framework. High Performance Liquid Chromatography (HPLC) analyses of the leakage of aldehyde **1** from an unwashed MOF sample showed the presence of **1** in solution already after few minutes. Samples analysed at later times indicated that the area of the aldehyde peak of **1** remained almost unchanged, due to the considerably higher amount of **1** present on the surface and immediately released in solution compared to the amount leaked from the inside of the MOF. On the other hand, the concentration of **1** in a washed MOF sample slowly increased over time, proving extraction of **1** from the MOF into the solution, with a significant diminution of the weakly coordinated aldehyde on the MOF surface *(*Figure 4-a*)*.

2.3. Quantification of the aldehyde in the different materials

In order to estimate the amount of aldehyde **1** included in the materials, two methods have been employed: leakage experiments followed by HPLC analysis and MOF digestion followed by NMR analysis. In the first method, the intensity of the absorption, and so the area of the aldehyde peak in the chromatogram, is proportional to its concentration in the liquid sample (Beer-Lambert law). However, it has been used only as an indirect method for a rough qualitative estimation, because the concentration will only represent the amount of aldehyde leaked from the MOF into the solution and not the amount present in the powder sample.

The second method is the MOF digestion by a media followed by NMR analyses of the resulting solution. The media dissolves the organic components of the MOF (linkers and aldehyde) while the inorganic portions precipitate as inorganic salts. NMR analysis allows to correlate the aldehyde signals with the signals coming from the linkers (Figure 4-c). This method can be considered a direct quantification of the amount of aldehyde in the material. With Zr-based MOFs, a basic digestion with NaOH in D_2O is normally employed. In our case, the Soai aldehyde **1** was found insoluble in the basic media. Instead, an acidic solution of 1% v/v D_3PO_4 in DMSO-d_6 was used as digestion media.

When analyses on the same materials have been made with the two methods, they have shown similar trends in the amount of aldehyde included (Figure 4-b). For instance, the inclusion process has been performed in MOFs with different linkers: pristine UiO-67, UiO-67 $bpy_{10\%}$, UiO-67 binaphtyl and UiO-66 (See SI). UiO-67 $bpy_{10\%}$ was the UiO-MOF in which the highest amount of aldehyde **1** was allocated. On the other hand, UiO-66 was the one with the lowest amount of guest inclusion. Interestingly UiO-67 binaphtyl, characterized by a much-hindered cage, was found able to allocate a slightly higher amount of Soai aldehyde compared to UiO-67. This

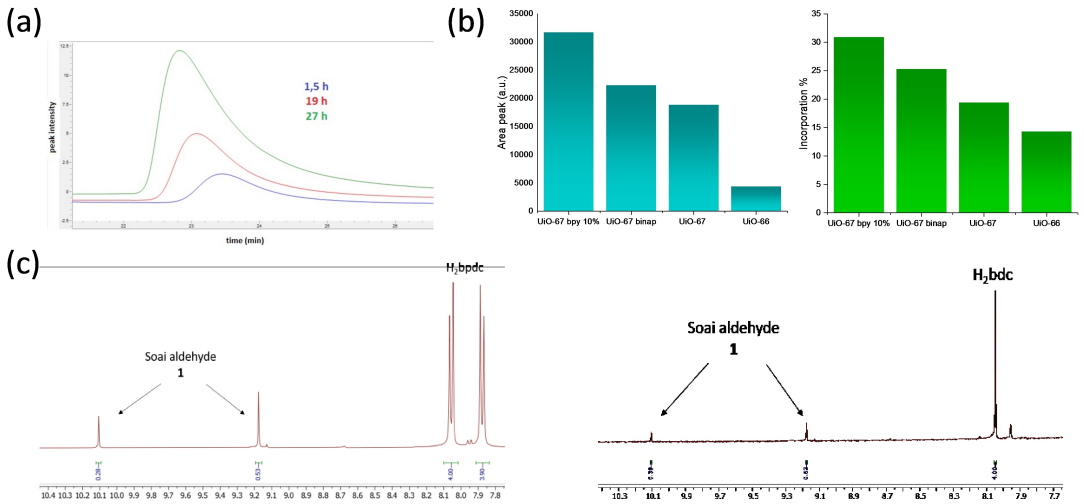

Figure 4. (a) Leakage experiments from washed UiO-67. **(b)** HPLC (left) and NMR (right) dual quantification of **1** in different UiO-MOFs. **(c)** ^{1}H NMR of digested UiO-67 (left) and UiO-66 (right) in acidic solution of 1% D_3PO_4 in DMSO-d_6.

could be explained by π-π interactions between the naphtyl rings of the linker and the pyrimidine rings of aldehyde **1**.

2.4. Analyses on the MOF materials after inclusion of Soai aldehyde 1

It was crucial to obtain a crystalline material after the inclusion step. In amorphous MOFs Soai aldehyde **1** would probably have been allocated in only certain areas of the MOF framework. Consequently, in such a MOF it is difficult to exploit the confinement effect and to evaluate the influence of the framework on the reactions. PXRD (Powder X-Ray Diffraction) analysis of the MOF with included Soai aldehyde showed no loss in crystallinity compared to the starting material (See SI).

ATR-IR analysis (Attenuated Total Reflectance Infrared Spectroscopy) was performed on the materials. A series of diagnostic signals indicate the presence of aldehyde **1** in the framework of UiO-67 (red line of Figure 5-a). The signal at 1700 cm^{-1} can be attributed to the stretching of the carbonyl group of the Soai aldehyde **1**, furthermore the peak around 2200 cm^{-1} can be attributed to the C–N stretching of the aromatic ring while the C–H stretching of the terbutyl/isopropyl groups can be observed below 3000 cm^{-1}. Interestingly, the O–H stretching of the hydroxyl groups of the clusters below 3700 cm^{-1} in the pristine material are perturbed in the UiO-67 after inclusion. This is a possible confirmation of the interaction with **1** predicted by the DFT calculations. The ATR-IR analyses have also been performed on a sample of UiO-66 before and after the inclusion (Figure 5-b). The previously discussed signals of the aldehyde in the framework are present in UiO-66 after the inclusion treatment (blue line). Moreover, aldehyde **1** seems to be allocated in a different position in the framework of UiO-66 compared to UiO-67. This can be supported by the hydroxyl groups of the clusters not being perturbed in the sample after inclusion, meaning that the aldehyde is not interacting with them. Again, the results are in agreement with the DFT calculations.

2.5. Vapour phase reaction set-ups

Recently, we have reported two set-ups to perform vapour-phase reactions.[8b] These set-ups have been employed for the experiments described in the next section. In the first set-up, the Soai reagent (pristine **1** or included in the MOFs) is placed on the top of a cylindrical glass support, arranged inside a glass vial. In the second set-up, three cylindrical glass supports containing the reagent were located in a bigger vial, in an attempt to secure that the conditions of the gas phase reaction were the same in all the samples. In both cases, $Zn(i\text{-}Pr)_2$ solution in toluene is added on the bottom under inert atmosphere and the vial is immediately sealed (See SI, Section 1). The first set-up was employed for the experiments of Table 2, while the second set-up for all the other reported experiments.

3. Results and Discussion

3.1. Preliminary results

All reactions were conducted at room temperature, and stopped after 24 hours if not specified otherwise, with reaction conditions varying in concentration of substrate, nature and size of the MOF and potentially relevant chiral trigger alkanol **2**. Firstly, our interest has been focused on the reactivity of the Soai aldehyde **1** in three different materials. We began our studies with a set of gas phase reactions with pristine Soai aldehyde **1**, unwashed UiO-67 with included **1** and washed UiO-67 with included **1** respectively. Under these different conditions, subjecting aldehyde **1** to reaction with iPr_2Zn vapour allowed symmetry breaking by absolute asymmetric alkylation

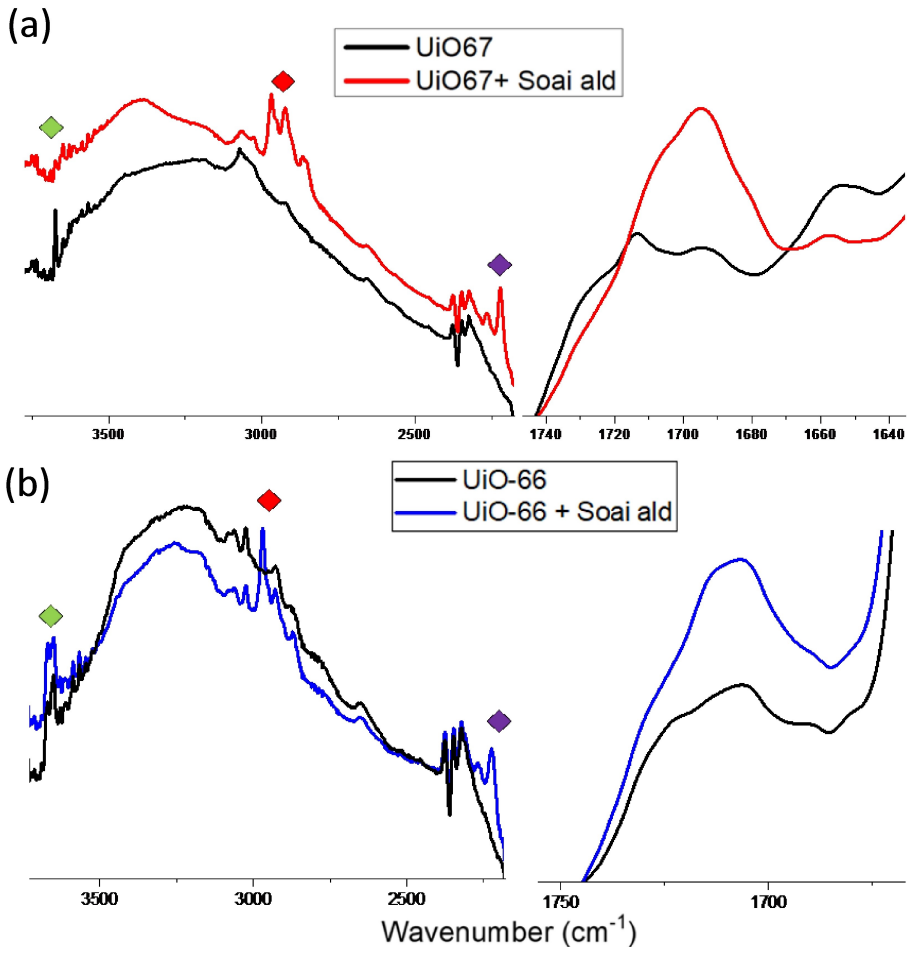

Figure 5. ATR-IR of UiO-66 and UiO-66 after inclusion of aldehyde **1**. On the left, stretching of the hydroxyl groups (in green), stretching of the terbutyl/isopropyl groups (in red), stretching of the C–N of the ring (in purple). On the right, stretching of the carbonyl group.

to afford alkanol **2**. This observation was expected for pristine substrate **1**, based on previous literature, although in the present experiment a remarkable 88% *ee* is reached. However, this amplification is affected by the confinement conditions in MOF. In terms of conversion, the washed MOF sample provided a slightly lower conversion compared to the other two samples. In contrast, the final ee% of the unwashed MOF was more similar to the pristine Soai powder, even with an opposite handedness of the product (*S*)-**2** in 70% ee, whereas the washed MOF sample yielded a lower amplification of (*R*)-**2** with 38% ee *(*Table 1*)*.

The results in Table 1 are in line with those obtained with the leakage experiments in washed *vs.* unwashed UiO-67. In the unwashed sample the Soai aldehyde **1** is confined in the framework but at the same time an excess of aldehyde **1** is also present on the surface of the MOF. The latter corresponds to surface confinement which reacts in a similar way to the pristine powder of **1**. In contrast, after several washes there is little or no Soai aldehyde present on the surface and the UiO-67 MOF contains only confined **1**. Thus, the conversion of Soai aldehyde **1** into Soai alcohol **2** takes place only within the pores of the MOF. A second series of experiments has been performed exposing the same substrate, washed UiO-67, but in different scale, to $Zn(i\text{-}Pr)_2$ vapors. The results shown in Table 1 reveal comparable conversions and final ee% obtained after reaction.

On the basis of these *observations*, it was reasonable to think that instead of the amount of MOF powder with included **1**, the different ratio of **1** in the MOF could play a crucial role in the reaction outcome. However, as shown in in table 1, similar results were obtained in terms of conversion and amplification. UiO-67 with different loadings of included aldehyde **1** have been obtained and tested to the reaction. The amount of aldehyde **1**, confined in **MOF**, has been evaluated by NMR analysis. Even different amounts of aldehyde **1** in the framework seem to not play a role in the final outcome of the reaction. This suggests that such low loadings are not significant to make a difference in the reaction outcome, even if the MOFs has different concentrations of aldehyde **1**. Probably similar experiments with MOFs at higher inclusion of aldehyde **1** (3% or 100%) would give different results, but the difficulty to reach such high inclusion percentages makes it problematic to prove the assumption.

To better understand what could influence the outcome of the reaction in terms of handedness and conversion, a mixture of Soai aldehyde **1** and Soai alcohol **2** has been included in three samples of UiO-67. The initial solution for the inclusion

Table 1. Variations of reaction conditions.

Entry[a]	Initial reaction conditions		5-Pyridyl Alkanol **2** Configuration	ee [%][b] [c]	Conv. [%]
1	Sample Form for **1**	Pristine	*R*	88	99
2		Unwashed UiO-67	*S*	70	98
3		Washed UiO-67	*S*	38	82
4	Load of UiO-67 including **1**[d]	1.5 mg	*R*	43	95
5		3 mg	*R*	43	91
6		6 mg	*R*	46	88
7	Inclusion level of **1** in UiO-67[e]	2.5%	*R*	28	69
8		10.5%	*R*	22	70
9		11%	*R*	23	72
10	Chiral trigger[f]	(*R*)-**2** 15% ee	*R*	50	81
11		(*S*)-**2** 50% ee	*S*	39	80
12		(*R*)-**2** 96% ee	*R*	69	84

[a] A typical procedure for vapour on solid alkylation is described in the Supporting information. [b] Determined on crude product. [c] The ee was determined using HPLC employing a chiral stationary phase. [d] Vapour phase reaction on different amount of washed UiO-67. [e] UiO-67 with different load of **1** determined by NMR. [f] Alkanol trigger **2** and aldehyde **1** were mixed together before inclusion into MOF.

had an aldehyde:alcohol ratio of 1:0,2, but in two out of three samples the ratio of the included species was found lower. The samples have then been tested to vapour phase reaction and the results are shown in Table 1.

The alcohol included was able to direct the handedness of the new formed alcohol, but the amplification of *ee* was seen only in the first case. The amount of alcohol **2** in the framework is lower compared to aldehyde **1**, and it can be speculated that it won't be present in all MOF crystals and all framework cavities. There will be reaction cycles in certain crystals whose outcome in terms of handedness of alcohol **2** will be dictated by the presence of the already included alcohol, and "competing" reaction cycles that will develop under absolute conditions (without alcohol **2**) with a random distribution of enantiomers for the product, The result of this multi-site reaction system, enhanced by the diffusion problems of the reaction intermediates, is that the presence of the reaction catalyst is almost uninfluential.

3.2. Kinetic plots of the gas phase reactions

Three samples consisting of pristine Soai aldehyde, Soai aldehyde included in UiO-67 and Soai aldehyde included in UiO-66 have been placed in several glass vials, the addition of the $Zn(i\text{-}Pr)_2$ solution has been performed at the same time and the reaction has been stopped at fixed time intervals. Conversion and *ee* amplification obtained in the three different samples have been measured with HPLC and plotted in Figure 6-a and Figure 6-b. These show that after reaction initiates, conversion is more significant in pristine and confined Soai **1** in UiO-67 to reach 80%, while reaction in UiO-66 levels-off at 40% conversion. While symmetry breaking remains a random event, amplification of **2** up to 80% *ee* is favoured by abundance of starting substrate **1** at the expense of confined reactions, ranging between 34–40% ee.

In the same way the kinetic profile of the reaction has been compared in pristine Soai aldehyde, Soai aldehyde included in UiO-67 and Soai aldehyde included in UiO-67 $bpy_{10\%.}$ (Figure 6-c and Figure 6-d). The kinetic plot of the conversion demonstrates an initial higher rate for the reaction confined in both the UiO-67 in respect to the pristine Soai aldehyde. The observed reactivity may find explanation in the ability to capture and diffuse vapors of $Zn(i\text{-}Pr)_2$ within the cavities of the solid framework, which is dependent of the size of the MOF and may influence its availability to react with aldehyde. Moreover, introduction of the bipyridine linker in the UiO-67 $bpy_{10\%}$ provides an additional coordination site for the organozinc reagent, which allows a controlled diffusion as compared to UiO-67. Even small cavities of the UiO-66 are able to allocate the oligomers of the catalytic cycle, although with lower conversions. Another significant aspect for the reactivity is related to the boundary conditions of supply of aldehyde, i.e., available amount of **1** considered in terms of concentration in the solid, that can impact the ability to form different oligomers, both in nature and size. Thus, with deficient aldehyde **1** short oligomers may also be autocatalytically active with high rate but lower enantioselectivity. In contrast, a higher concentration of aldehyde is in favour of higher and more enantioselective oligomers resulting in higher enantiopurity of alkanol.[25] However, mobility between the cavities of the solid can induce dissociation of such large entities into shorter aggregates to pass through the openings, such as in UiO-66.

The level of amplification was always found lower in the MOFs as compared to the pristine aldehyde **1**, a consequence of the limited space available for the reaction to propagate due to the confinement in the framework. However, sampling at early conversion rates of the reactions in MOF did not provide measurable traces of alkanol **2**. Therefore, the typical sigmoidal shape usually observed in the case of the Soai reaction could not be reproduced. Perhaps most important, is that in all cases, amplification keeps pace after symmetry breaking, but with less significant increments throughout the process, in contrast to the exponential amplification of typical Soai reaction.

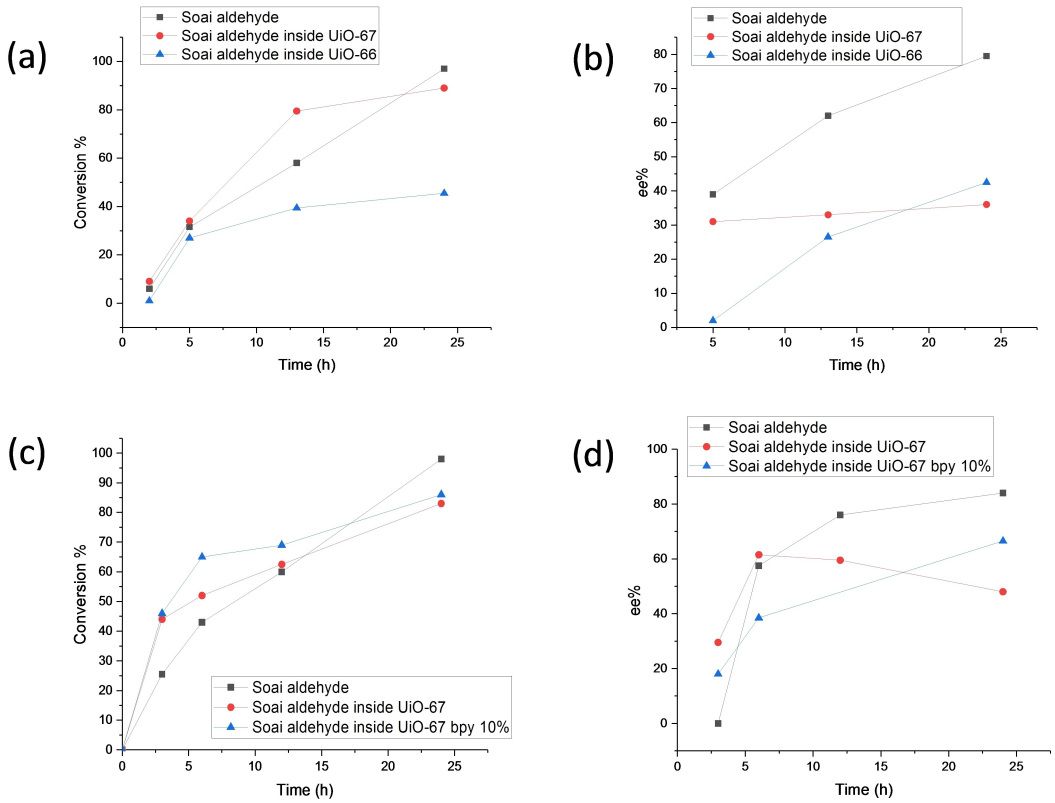

Figure 6. Effect of MOF size on conversion **(a)** and ee amplification **(b)** over time; Effect of chemical structure of MOF on conversion **(c)** and ee amplification **(d)** over time.

3.3. Screening of different UiO MOFs

To make sure the symmetry breaking in MOFs follows a random event and allows for absolute asymmetric synthesis, we conducted the exposure experiments by using MOFs and Zn(i-Pr)$_2$ different origins. Thus, a number of inclusion forms of aldehyde **1** were screened for the vapour phase reactions with three different Zn(i-Pr)$_2$ batches. The zinc solutions were added at the same time and the reactions stopped for every run after 7 days. The results are shown in Table 2 below.

In absence of chiral inductor, alkylation of aldehyde **1** in UiO MOFs provide enantiomers of the alcohol **2** at random, a characteristic feature of an Absolute Asymmetric Synthesis. The low amplification level of *ee* in MOFs compared to the pristine Soai aldehyde can only result from the confinement effect of the framework of the MOF: such a constraint allows for limited diffusion of the oligomeric species involved in the autocatalytic cycles. Thus, autocatalysis is probably confined to several reaction compartments, and the final observed *ee* consists of a sum of the total autocatalytic cycles occurring in multiple local sites of the MOF. In contrast, in the pristine Soai all equivalents of aldehyde **1** are part of a continuum allowing for a same autocatalytic cycle. The rising *ee* may be reflecting the local chirality in UiO-MOF series. Considering the 15 reactions performed in Table 2, five yielded (*S*)-**2**, while the other ten yielded (*R*)-**2**. This could lead to think of a *pro-R* orientation of the Soai aldehyde included in the MOF. Based on the recent report from Soai *et al.*, and despite the presence of a

Table 2. Screening of different UiO MOFs to the gas phase reaction.

Entry	Soai reagent	%	Zinc batch **1**	Zinc batch **2**	Zinc batch **3**
1	Pristine	Conv.	99	99	99
		ee	93 (*S*)	92 (*R*)	94 (*R*)
2	UiO-67	Conv.	93	93	92
		ee	23 (*R*)	30 (*R*)	14 (*S*)
3	UiO-67 bpy$_{10\%}$	Conv.	81	86	89
		ee	19 (*R*)	26 (*S*)	48 (*R*)
4	UiO-67 binaphtyl	Conv.	80	72	82
		ee	21 (*R*)	43 (*S*)	28 (*R*)
5	UiO-66	Conv.	55	51	43
		ee	32 (*R*)	35 (*R*)	16 (*S*)

preferential location for the aldehyde in UiO-MOFs, aldehyde **1** is randomly distributed within the framework in a disordered manner.[8a] Even if (*R*)-**2** may seem to prevail, this could be just due to the small number of experiments performed.

3.4. Analyses on the materials after the vapour-phase reactions

Two samples of pristine UiO-67 $bpy_{10\%}$ and UiO-67 $bpy_{10\%}$ with included aldehyde **1** were subjected to the vapour phase reaction. Figure 7-a depicts the Capillary X-ray diffraction (C-XRD) pattern of both the material which resembles the C-XRD of pristine MOF. This shows that both materials maintain crystallinity after reaction. The Zr cluster ($Zr_6O_6(bpdc)_6$) contains μ_3-OH. This site may provide an additional anchoring point for $Zn(iPr)_2$ during the vapour phase reaction (Figure 8).[26] Closer analyses at the XRD diffractograms did not show any interaction between zinc reagents and the clusters. Moreover, Soai has shown that the presence of additives containing hydroxyl moieties does not interfere with the autocatalytic process and the asymmetric amplification.[27]

ATR-IR analysis has also been carried out on the MOF samples after reaction. Confronting the spectra of the three materials in Figure 7-b, the C=O stretching of the carbonyl group of aldehyde **1** at 1700 cm^{-1}, (totally absent in the parent material), almost disappears in the UiO-67 after vapour phase reaction. Although diagnostic signals of the alcohol group of **2** are not possible to detect (hidden by peaks of the carboxylate linkers), other signals, common to both **1** and **2** are visible: the C–H stretching of the terbutyl/isopropyl groups below 3000 cm^{-1} and the C–N stretching of the ring at 2200 cm^{-1}. The stretching of the O–H groups above 3500 cm^{-1}, present in the pristine material and perturbed in the material after the inclusion, is still perturbed after the vapour phase reaction. This hints that alcohol **2** is still allocated on the cluster. The ATR-IR analysis alone indicates that a similar molecule to aldehyde **1** is present in the material, and they complement nicely the results obtained through other techniques and described above.

4. Conclusions

The present study shows that, despite the confined environment of a crystalline sponge, active autocatalytic species still can form in the Soai reaction and symmetry breaking with amplification is observed. Thus, under heterogenous conditions and in absence of chiral polarization, absolute asymmetric synthesis promotes formation of Soai alkanol **2** by reaction of $Zn(iPr)_2$ vapor with aldehyde **1** encapsulated in UiO-MOF series. In contrast to traditional asymmetric synthesis, and given that all MOFs used in these experiments are *"achiral"*, the present reaction set-up exemplifies a closed system far from equilibrium reaching a stable non-stationary phase. Somehow, reactions

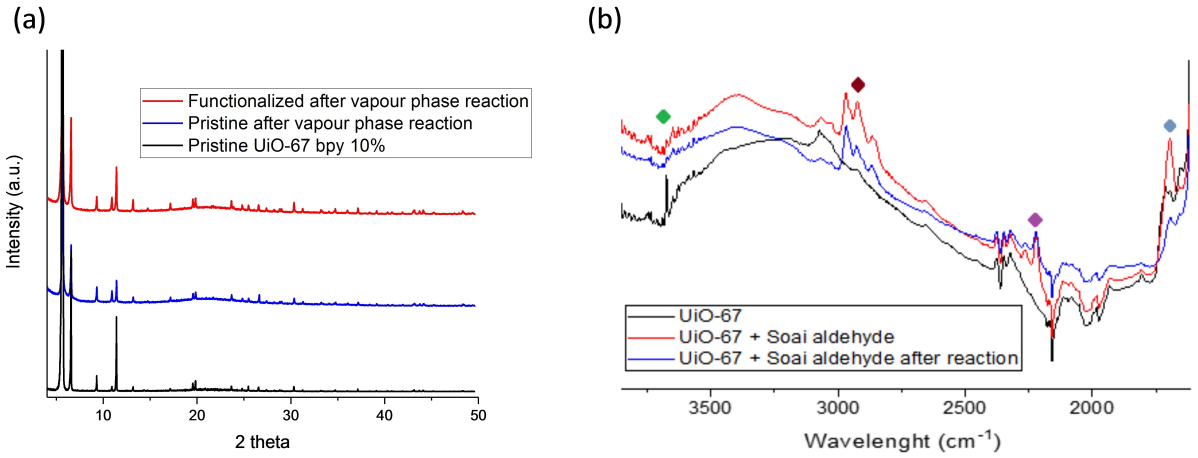

Figure 7. (a) XRD analysis on the MOFs. **(b)** IR analysis on the UiO-67 after vapour phase reaction showing stretching of the: hydroxyl groups (green), terbutyl group (red), C–N in pyrimidine ring (purple), carbonyl group (blue).

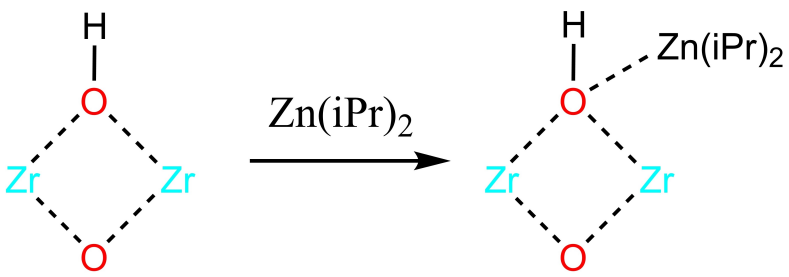

Figure 8. Possible interaction between $Zn(i\text{-}Pr)_2$ and the Zr–O moiety of the MOF cluster.

conducted in the UiO-67 MOF were faster than in smaller UiO-66 or in pristine materials. In contrast to pristine solid **1**, moderate amplification of *ee* was observed for reactions conducted in UiO-MOFs as confinement restricts diffusion of chiral active oligomers of Zn-**2** within the solid. Also, the boundary conditions in supply of reactants causes formation of different aggregates with different autocatalytic performances resulting in changing reaction rates and *ee*. ATR-IR data localize aldehyde **1** in close proximity to the Zr-cluster, in agreement with predicted coordination by DFT calculations, which is confirmed by similar localization of product **2** after reaction. Also, the crystallinity of the MOF is well preserved after vapour phase reaction with $Zn(iPr)_2$. To our knowledge this is the first example of symmetry breaking for autocatalytic amplification in such confined environment.

Conflict of Interest

The authors declare no conflict of interest.

Keywords: UiO-MOF · Autocatalysis · Symmetry breaking · Amplification · Chirality

[1] a) K. Mislow, *Collect. Czech. Chem. Commun.* **2003**, *68*, 849–864; b) M. Bolli, R. Micura, A. Eschenmoser, *Chem. Biol.* **1997**, *4*, 309–320; c) B. L. Feringa, R. A. van Delden, *Angew. Chem. Int. Ed.* **1999**, *38*, 3419–3438; d) S. Pizzarello, A. L. Weber, *Science (Washington, DC, U. S.)* **2004**, *303*, 1151; e) I. Weissbuch, M. Lahav, *Chem. Rev. (Washington, DC, U. S.)* **2011**, *111*, 3236–3267; f) J. S. Siegel, *Chirality* **1998**, *10*, 24–27; g) J. M. Ribo, C. Blanco, J. Crusats, Z. El-Hachemi, D. Hochberg, A. Moyano, *Chem. Eur. J.* **2014**, *20*, 17250–17271.
[2] a) A. J. Bissette, S. P. Fletcher, *Angew. Chem. Int. Ed.* **2013**, *52*, 12800–12826; *Angew. Chem.* **2013**, *125*, 13034–13061; b) D. G. Blackmond, *Chem. Rev.* **2020**, *120*, 4831–4847.
[3] F. C. Frank, *Biochim. Biophys. Acta* **1953**, *11*, 459–463.
[4] K. Soai, T. Shibata, H. Morioka, K. Choji, *Nature* **1995**, *378*, 767–768.
[5] a) I. Sato, H. Urabe, S. Ishiguro, T. Shibata, K. Soai, *Angew. Chem. Int. Ed.* **2003**, *42*, 315–317; *Angew. Chem.* **2003**, *115*, 329–331; b) T. Shibata, S. Yonekubo, K. Soai, *Angew. Chem. Int. Ed.* **1999**, *38*, 659–661; *Angew. Chem.* **1999**, *111*, 746–748.
[6] a) K. Soai, T. Kawasaki, A. Matsumoto, *Acc. Chem. Res.* **2014**, *47*, 3643–3654; b) K. Soai, T. Kawasaki, A. Matsumoto, *Tetrahedron* **2018**, *74*, 1973–1990.
[7] a) D. A. Singleton, L. K. Vo, *Org. Lett.* **2003**, *5*, 4337–4339; b) K. Soai, I. Sato, T. Shibata, S. Komiya, M. Hayashi, Y. Matsueda, H. Imamura, T. Hayase, H. Morioka, H. Tabira, J. Yamamoto, Y. Kowata, *Tetrahedron: Asymmetry* **2003**, *14*, 185–188.
[8] a) Y. Kaimori, Y. Hiyoshi, T. Kawasaki, A. Matsumoto, K. Soai, *Chem. Commun.* **2019**, *55*, 5223–5226; b) G. Rotunno, D. Petersen, M. Amedjkouh, *ChemSystemsChem* **2020**, *2*, e1900060.
[9] a) B. L. Feringa, R. A. van Delden, *Angew. Chem. Int. Ed.* **1999**, *38*, 3418–3438; *Angew. Chem.* **1999**, *111*, 3624–3645; b) K. Mislow, *Collect. Czech. Chem. Commun.* **2003**, *68*, 849.
[10] a) D. G. Blackmond, C. R. McMillan, S. Ramdeehul, A. Schorm, J. M. Brown, *J. Am. Chem. Soc.* **2001**, *123*, 10103–10104; b) F. G. Buono, D. G. Blackmond, *J. Am. Chem. Soc.* **2003**, *125*, 8978–8979.
[11] a) I. D. Gridnev, J. M. Serafimov, J. M. Brown, *Angew. Chem. Int. Ed.* **2004**, *43*, 4884–4887; *Angew. Chem.* **2004**, *116*, 4992–4995; b) I. D. Gridnev, J. M. Brown, *Proc. Natl. Acad. Sci. USA* **2004**, *101*, 5727; c) J. Klankermayer, I. D. Gridnev, J. M. Brown, *Chem. Commun.* **2007**, 3151–3153; d) I. D. Gridnev, J. M. Serafimov, H. Quiney, J. M. Brown, *Org. Biomol. Chem.* **2003**, *1*, 3811–3819.
[12] M. E. Noble-Terán, J.-M. Cruz, J.-C. Micheau, T. Buhse, *ChemCatChem* **2018**, *10*, 642–648.
[13] I. D. Gridnev, A. K. Vorobiev, *ACS Catal.* **2012**, *2*, 2137–2149.
[14] a) L. Schiaffino, G. Ercolani, *Angew. Chem. Int. Ed.* **2008**, *47*, 6832–6835; *Angew. Chem.* **2008**, *120*, 6938–6941; b) L. Schiaffino, G. Ercolani, *Chemistry* **2010**, *16*, 3147–3156; c) G. Ercolani, L. Schiaffino, *J. Org. Chem.* **2011**, *76*, 2619–2626.
[15] A. Matsumoto, T. Abe, A. Hara, T. Tobita, T. Sasagawa, T. Kawasaki, K. Soai, *Angew. Chem. Int. Ed.* **2015**, *54*, 15218–15221; *Angew. Chem.* **2015**, *127*, 15433–15436.
[16] T. Gehring, M. Quaranta, B. Odell, D. G. Blackmond, J. M. Brown, *Angew. Chem. Int. Ed.* **2012**, *51*, 9539–9542, S9539/9531-S9539/9541.
[17] O. Trapp, S. Lamour, F. Maier, A. F. Siegle, K. Zawatzky, B. F. Straub, *Chem. - Eur. J.* **2020**, *26*, 15871–15880.
[18] a) E. Doka, G. Lente, *J. Am. Chem. Soc.* **2011**, *133*, 17878–17881; b) O. Fulop, B. Barabas, *J. Math. Chem.* **2016**, *54*, 10–17; c) B. Barabas, R. Kurdi, C. Zucchi, G. Palyi, *Chirality* **2018**, *30*, 913–922; d) B. Barabas, J. Toth, G. Palyi, *J. Math. Chem.* **2010**, *48*, 457–489; e) D. G. Blackmond, *Tetrahedron: Asymmetry* **2006**, *17*, 584–589; f) J.-C. Micheau, C. Coudret, J.-M. Cruz, T. Buhse, *Phys. Chem. Chem. Phys.* **2012**, *14*, 13239–13248.
[19] S. V. Athavale, A. Simon, K. N. Houk, S. E. Denmark, *Nat. Chem.* **2020**, *12*, 412–423.
[20] a) Y. Kaimori, Y. Hiyoshi, T. Kawasaki, A. Matsumoto, K. Soai, *Chem. Commun.* **2019**, *55*, 5223–5226; b) T. Buhse, J.-M. Cruz, M. E. Noble-Terán, D. Hochberg, J. M. Ribó, J. Crusats, J.-C. Micheau, *Chem. Rev.* **2021**, *121*, 2147–2229.
[21] R. Batten Stuart, R. Champness Neil, X.-M. Chen, J. Garcia-Martinez, S. Kitagawa, L. Öhrström, M. O'Keeffe, M. Paik Suh, J. Reedijk in *Terminology of metal–organic frameworks and coordination polymers (IUPAC Recommendations 2013), Vol. 85* **2013**, p. 1715.
[22] a) A. Gheorghe, M. A. Tepaske, S. Tanase, *Inorg. Chem. Front.* **2018**, *5*, 1512–1523; b) X. Li, J. Wu, C. He, Q. Meng, C. Duan, *Small* **2019**, *15*, 1804770; c) S. Bhattacharjee, I. M. Khan, X. Li, Q.-L. Zhu, X.-T. Wu, *Catalysts* **2018**, *8*; d) A. V. Artem'ev, V. P. Fedin, *Russ. J. Org. Chem.* **2019**, *55*, 800–817; e) Y. Liu, W. Xuan, Y. Cui, *Adv. Mater.* **2010**, *22*, 4112–4135.
[23] J. H. Cavka, S. Jakobsen, U. Olsbye, N. Guillou, C. Lamberti, S. Bordiga, K. P. Lillerud, *J. Am. Chem. Soc.* **2008**, *130*, 13850–13851.
[24] a) L. M. Hayes, C. E. Knapp, K. Y. Nathoo, N. J. Press, D. A. Tocher, C. J. Carmalt, *Cryst. Growth Des.* **2016**, *16*, 3465–3472; b) M. Hoshino, A. Khutia, H. Xing, Y. Inokuma, M. Fujita, *IUCrJ* **2016**, *3*, 139–151; c) Y. Inokuma, S. Yoshioka, J. Ariyoshi, T. Arai, Y. Hitora, K. Takada, S. Matsunaga, K. Rissanen, M. Fujita, *Nature* **2013**, *495*, 461–466; d) J.-S. Qin, S. Yuan, A. Alsalme, H.-C. Zhou, *ACS Appl. Mater. Interfaces* **2017**, *9*, 33408–33412.
[25] J. M. Brown, I. Gridnev, J. Klankermayer in Asymmetric autocatalysis with organozinc complexes; Elucidation of the reaction pathway, Vol. 284 (Ed. K. Soai), **2008**, pp. 35–65.
[26] a) L. C. Gallington, I. S. Kim, W.-G. Liu, A. A. Yakovenko, A. E. Platero-Prats, Z. Li, T. C. Wang, J. T. Hupp, O. K. Farha, D. G. Truhlar, A. B. F. Martinson, K. W. Chapman, *J. Am. Chem. Soc.* **2016**, *138*, 13513–13516; b) I. S. Kim, J. Borycz, A. E. Platero-Prats, S. Tussupbayev, T. C. Wang, O. K. Farha, J. T. Hupp, L. Gagliardi, K. W. Chapman, C. J. Cramer, A. B. F. Martinson, *Chem. Mater.* **2015**, *27*, 4772–4778.
[27] a) T. Kawasaki, Y. Wakushima, M. Asahina, K. Shiozawa, T. Kinoshita, F. Lutz, K. Soai, *Chem. Commun.* **2011**, *47*, 5277–5279; b) T. Shibata, H. Tarumi, T. Kawasaki, K. Soai, *Tetrahedron: Asymmetry* **2012**, *23*, 1023–1027.

Manuscript received: April 19, 2021
Revised manuscript received: June 30, 2021
Accepted manuscript online: July 11, 2021
Version of record online: July 21, 2021